Planar glass waveguide ring resonators with gain

Hsien-kai Hsiao and K. A. Winick*

Department of Electrical Engineering and Computer Science, University of Michigan, 1301 Beal Avenue, Ann Arbor, MI 48109-2122, USA
**Corresponding author: winick@umich.edu*

Abstract: The frequency resolution of an active waveguide ring resonator spectrometer is fundamentally limited by spontaneous emission noise produced by the gain medium. A closed-form expression for this resolution is derived, and the result is used to determine the minimum, rms, angular rotation rate, random walk error achievable by an active ring resonator gyroscope. An active waveguide ring resonator is demonstrated in a neodymium-doped glass, and a finesse of 250 at a signal wavelength of 1060 nm is achieved for the 1.6 cm diameter ring under laser diode pumping. This finesse corresponds to an effective propagation loss on the order of 0.013 dB/cm, which is the lowest value reported to date for rings of this size.

OCIS codes: (140.4780) Optical resonators; (060.2800) Gyroscopes; (130.2755) Glass waveguides; (230.3120) Integrated optics devices; (280.4788) Optical sensing and sensors; (300.6190) Spectrometers.

References and links

1. C.K. Madsen, G. Lenz, A. J. Bruce, M. A. Cappuzzo, L. T. Gomez and R. E. Scotti, "Integrated all-pass filters for tunable dispersion and dispersion slope compensation," Photon. Technol. Lett. **11**, 1623-1625 (1999).
2. S. T. Chu, B.E. Little, W. Pan, T. Kaneko and Y. Kokubun, "A second-order filter response from parallel coupled glass microring resonators," Photon. Technol. Lett. **11**, 1426-1428 (1999).
3. G. Priem, P. Dumon, W. Bogaerts, D. Van Thourhout, G. Morthier and R. Baets, "Optical bistability and pulsating behavior in silicon-on-insulator ring resonator structures," Opt. Express **13**, 9623-9628 (2005).
4. Q. Xu and M. Lipson, "All-optical logic based on silicon micro-ring resonators," Opt. Express **15**, 924-929 (2007).
5. A. Ksendzov and Y. Lin, "Integrated optics ring-resonator sensors for protein detection," Opt. Lett. **30**, 3344-3346 (2005).
6. P. Mottier and P. Pouteau, "Solid state optical gyrometer integrated on silicon," Electron. Lett. **33**, 1975-1977 (1997).
7. J. Haavisto and G. A. Pajer, "Resonance effects in low-loss ring waveguides," Opt. Lett. **5**, 510-512 (1980).
8. R. G. Walker and C. D. W. Wilkinson, "Integrated optical ring resonators made by silver ion-exchange in glass," Appl. Opt. **22**, 1029-1035 (1983).
9. G. Li, K. A. Winick, H. C. Griffin and J. Hayden, "Systematic modeling study of channel waveguide fabrication by thermal silver ion exchange," Appl. Opt. **45**, 1743-1755 (2006).
10. R. Adar, M. R. Serbin and V. Mizrahi, "Less than 1 dB per meter propagation loss of silica waveguides measured using a ring resonator," J. Lightwave Technol. **12**, 1369-1372 (1994).
11. T. Kitagawa, K. Hattori, Y. Hibino and Y. Ohmori, "Laser Oscillation in Erbium-Doped Silica-Based Planar Ring Resonators," *in Proceedings of 18th European Conf. on Optical Commun. (ECOC)*, (1992), Th PD-II.5, pp. 907-910.
12. W. Sohler, B. K. Das, D. Dey, S. Reza, H. Suche and R. Ricken, "Erbium-doped lithium niobate waveguide lasers," IEICE Trans. Electron. **E88-C**, 990- 997 (2005).
13. T. A. Dorschner, H. A. Haus, M. Holz I. W. Smith, H. Statz, "Laser gyro at quantum limit," J. Quantum Electron. **QE-16**, 1376-1379 (1980).
14. L. F. Stokes, M. Chodorow and H. J. Shaw,"All-single-mode fiber resonator," Opt. Lett. **7**, 288-290 (1982).

#87963 - $15.00 USD Received 27 Sep 2007; revised 3 Dec 2007; accepted 5 Dec 2007; published 13 Dec 2007

15. S. Ezekiel, S. P. Smith and F. Zarinetchi, "Basic principles of fiber-optic gyroscopes," in *Optical fiber Rotation Sensing*, W. K. Burns, ed., (Academic Press, NY, 1994), Chap. 1.
16. S. Ezekiel and S. R. Balsamo, "Passive ring resonator laser gyroscope," Appl. Phys. Lett. **30**, 478-480 (1977).
17. R. E. Meyer, S. Ezekiel, D. W. Stowe and V. J. Tekippe, "Passive fiber-optic ring resonator for rotation sensing," Opt. Lett. **8**, 644-646 (1983).
18. K. Suzuki, K. Takiguchi and K. Hotate, "Monolithically integrated resonator microoptic gyro on silica planar lightwave circuit," J. Lightwave Technol. **18**, 66-72 (2000).
19. H. Ma, X. Zhang, Z. Jin and C. Ding, "Waveguide-type optical passive resonator gyro using phase modulation spectroscopy technique," Optical Engineering Letters **45**, 080506-1 – 080506-3 (2006).
20. H. Okamura and K Iwatsuki, "A finesse-enhanced Er-doped-fiber ring resonator," J. Lightwave Technol. **9**, 1554-1560 (1991).
21. J. T. Kringlebotn, "Amplified fiber ring resonator gyro," Photon. Technol. Lett. **4**, 1180-1183 (1992).
22. J. T. Kringlebotn, P. R. Morkel, C. N. Pannell, D. N. Payne and R. I. Laming, "Amplified fibre delay line with 27 000 recirculations," Electron. Lett. **28**, 201-202 (1992).
23. W. T. Silfvast, "Radiation and thermal equilibrium," in *Laser Fundamentals*, (Cambridge University Press, 2004), Chap. 6.
24. W. T. Silfvast, "Conditions for producing a laser," in *Laser Fundamentals*, (Cambridge University Press, 2004), Chap. 7.

1. Introduction

Planar integrated optic ring resonators have been well-studied and find a host of applications in both telecommunications and sensing. These include optical filtering [1,2], nonlinear optics [3], optical switching [4], chemical and biological sensing [5] and angular rotation rate sensing [6]. Many of these applications require a resonator of high finesse, and thus a resonator having low loss. When the application also necessitates the use of a large diameter ring, as is the case for an optical gyroscope rotation rate sensor, glass becomes an ideal substrate material because it permits the fabrication of very low loss waveguides.

The first planar ring resonator were reported by Haavisto and Pajer in polymethyl methacrylate films and this work was later extended to glass using ion exchange [7,8]. These resonators had large propagation losses on the order of 2 dB/cm. Losses of approximately of 0.1 dB/cm can now be achieved by ion exchange for ring radii on the order of 1 cm [9], and losses half as large have reported for similarly sized waveguide rings fabricated using CVD-deposited silica on silicon together with reactive ion etching of the waveguide structure [10]. Currently there are no known methods for achieving even lower loss value for rings of this size. Waveguide losses can be attributed primarily to inhomogenieties in the glass and/or surface roughness at the core-cladding interface. Both of these contributing factors can be reduced by decreasing the refractive index contrast between the core and cladding. Such a decrease, however, will result in significant bending losses unless the ring diameter is increased commensurately. It is possible, however, to reduce the effective resonator loss below the values quoted above by incorporating gain inside the ring. With the presence of gain, lasing in erbium-doped, planar, waveguide, ring resonators has been reported in both glass [11] and $LiNbO_3$ [12] substrates. When operated below the lasing threshold, these devices exhibited a modest reduction of their resonant bandwidths, and hence an increase in finesse.

The spectral resolution of a passive ring resonator is limited by shot noise and is a function of the finesse of the resonator and the input signal power level. When gain is added to the ring, the resolution is ultimately limited by spontaneous emission noise generated by the gain medium. We derive an expression for this resolution using an analysis previously developed for ring laser gyroscopes [13]. Our analysis shows that in the quantum limit with gain present, the spectral resolution decreases as one over the square root of the product of the finesses of the resonator measured with gain and without gain. We apply this result to determine the minimum, rms, angular rotation rate, random walk error achievable by an active, ring, resonator gyroscope in the quantum limit. A closed-form expression is also

#87963 - $15.00 USD Received 27 Sep 2007; revised 3 Dec 2007; accepted 5 Dec 2007; published 13 Dec 2007

derived for the absorbed pump power required by an active ring resonator gyroscope as a function of the launched signal power and the finesse.

Finally, we fabricate an active, waveguide, ring resonator in a neodymium-doped glass by ion exchange. When the neodymium gain medium is pumped by a laser diode, the finesse of the 1.6 cm diameter device increases from approximately 10 to 250 at a signal wavelength of 1060 nm, with the later finesse value corresponding to an effective propagation loss value of approximately 0.013 dB/cm. We believe that this is the lowest effective propagation loss and highest finesse reported to date for glass, waveguide, ring resonators of this size. We also observe gain saturation in this ring resonator as the launched signal power is increased, and we report lasing action at sufficiently high pump powers.

2. Equations of ring resonators

Consider the double-arm ring resonator shown in Fig. 1 below consisting of a circular ring located in close proximity to two straight waveguides that serve to couple light into and out of the ring.

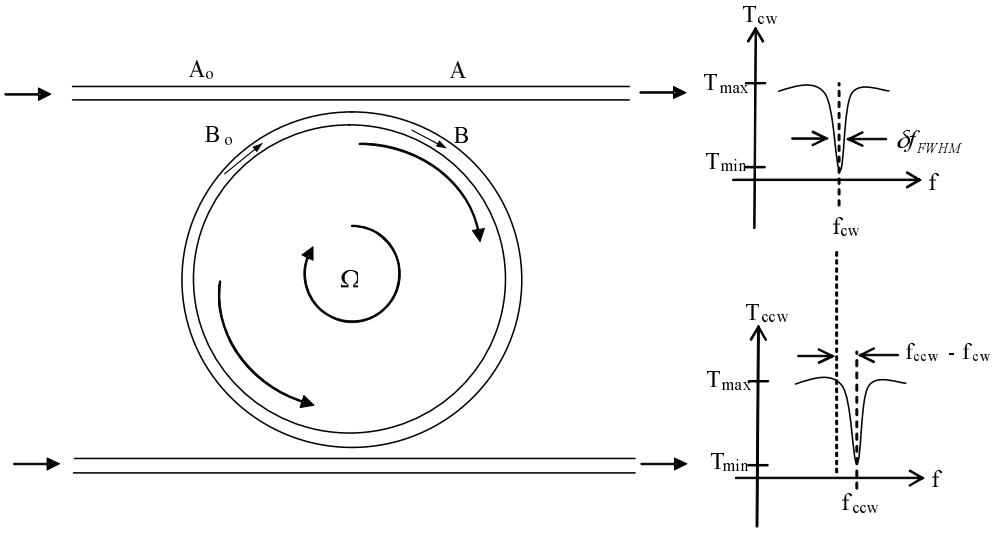

Fig. 1. Double arm ring resonator.

The electric field amplitudes, A, A_o, B and B_o, indicated in Fig. 1 can be related to one another by [14]

$$A = [A_o\sqrt{1-K_{cw}} - jB_o\sqrt{K_{cw}}] \tag{1}$$

$$B = [-jA_o\sqrt{K_{cw}} + B_o\sqrt{1-K_{cw}}] \tag{2}$$

$$B_o = B\sqrt{1-K_{ccw}}\exp(-\frac{\rho}{2}L - j\beta L) \tag{3}$$

where the coupling coefficient, K_{cw}, equals the fraction of optical power coupled into the ring from the top straight waveguides, L is the ring circumference, $1-\exp(-\rho L)$ equals the fraction of optical power lost upon one round-trip around the ring neglecting coupling losses to the straight waveguides and β is the propagation constant. For simplicity, we have

#87963 - $15.00 USD Received 27 Sep 2007; revised 3 Dec 2007; accepted 5 Dec 2007; published 13 Dec 2007

neglected any excess insertion losses associated with the coupling between the straight waveguides and the ring. Combining Eqs. (1)-(3) yields [14]

$$T(\phi) \equiv \left|\frac{A}{A_o}\right|^2 = 1 - \frac{(1-x^2)(1-y^2)}{(1-xy)^2 + 4xy\sin^2(\phi/2)} \tag{4}$$

where

$$x \equiv \sqrt{1-K_{ccw}}\,\exp(-\frac{\rho}{2}L) \tag{5}$$

$$y \equiv \sqrt{1-K_{cw}} \tag{6}$$

$$\phi \equiv \beta L = \frac{2\pi}{\lambda} N_{eff} L = \omega N_{eff} L/c \tag{7}$$

and the coupling coefficient, K_{ccw}, is the fraction of power coupled into the ring from the lower straight waveguide, λ is the free-space optical wavelength, ω is the optical frequency in rad/s and N_{eff} is the effective index of the guided mode. It will be assumed that light is launched into the ring only from the top straight waveguide. The transmittance T achieves a minima when ϕ equals an even integer multiple of π, corresponding to resonance in the ring. Using Eq. (4), the depth, D, of the resonance "dip" can be expressed as

$$\mathrm{D} \equiv \frac{T_{\max} - T_{\min}}{T_{\max}} = \frac{4xy(1-x^2)(1-y^2)}{(1-xy)^2(x+y)^2} \tag{8}$$

and the full-width of the resonance at half maximum, $\delta\phi_{FWHM}$, is equal to

$$\delta\phi_{FWHM} = 2\cos^{-1}\left[\frac{2xy}{1+x^2y^2}\right] \tag{9}$$

where this width is defined by the relationship

$$\frac{T(m\pi \pm \delta\phi_{FWHM}/2) - T_{\min}}{T_{\max} - T_{\min}} = 1/2 \tag{10}$$

The resonator finesse, F, is given by

$$F \equiv \frac{2\pi}{\delta\phi_{FWHM}} = \frac{2\pi c / N_{eff} L}{\delta\omega_{FWHM}} \tag{11}$$

where $\delta\omega_{FWHM}$ is the full-width-half-maximum of the resonance in rad/s. Eqs. (9) and (11) reduce to

$$F \approx \frac{\pi}{1-xy} \tag{12}$$

when $xy \approx 1$. The ratio of the power in the ring at resonance to that of the launched power in the straight waveguide is given by

$$\left|\frac{B}{A_o}\right|^2 = \frac{1-y^2}{[1-xy]^2} \tag{13}$$

According to Eq. (8) the dip will be maximized, achieving a value of 1, when x = y. Furthermore when $x = y \approx 1$, Eqs. (12) and (13) can be combined to yield

#87963 - $15.00 USD Received 27 Sep 2007; revised 3 Dec 2007; accepted 5 Dec 2007; published 13 Dec 2007

$$\left|\frac{B}{A_o}\right|^2 \approx F/\pi \tag{14}$$

By measuring the dip and finesse, both the coupling efficiency, K_{cw}, and $\sqrt{1-K_{ccw}}\exp(-\rho L/2)$ can be found using Eqs. (8), (9) and (11). When light is launched into the ring using only the bottom straight waveguide, all of the expressions given above remain valid provided that the two coupling coefficients, K_{cw} and K_{ccw}, are interchanged in these formula.

3. Spectral resolution of active ring resonator in quantum limit

Fig. 1 shows a double arm ring resonator functioning as a resonant optical gyroscope. Light is launched into each of the two resonator arms from separate laser sources and these two light beams counter-propagate along the ring. In the absence of rotation, the resonance frequencies for propagation in both the clockwise and counter-clockwise directions are given by

$$f_m = m\frac{c}{N_{eff}L} \tag{15}$$

where c is the vacuum speed of light and m is positive integer. Due to the Sagnac effect the resonant frequencies, $f_{m,cw}$ and $f_{m,ccw}$, corresponding to the counter-propagating beams will differ when angular rotation takes place about an axis normal to the plane of the ring. The difference in these frequencies is given by [15]

$$f_{m,ccw} - f_{m,cw} = \frac{4A}{\lambda_m L}\Omega \tag{16}$$

where A is the area enclosed by the ring, L is the perimeter of the ring, $\lambda_m = c/f_m$ and Ω is the angular rate of rotation around an axis normal to the plane of the ring. Thus the angular rotation rate can be determined by measuring this frequency difference. Resonant optical gyroscopes were proposed and demonstrated using fiber optics by Ezekiel et al. [16,17]. Several groups have implemented these gyros using planar, glass, waveguide rings in place of optical fibers [18,19].

The ultimate accuracy with which the frequency difference, $f_{m,ccw} - f_{m,cw}$, can be measured using a passive resonant optical gyro is limited by shot-noise and is given by [17]

$$\begin{aligned}\delta\Omega_{rms} &\approx \left(\frac{\lambda_m L}{4A}\right)\left[\frac{\sqrt{2}\delta\omega_{FWHM}/(2\pi)}{[\eta_D(P_{in}/hf_m)\tau_{\text{int}}]^{1/2}}\right] \\ &= \left(\frac{\lambda_m c}{4AN_{eff}}\right)\left[\frac{\sqrt{2}}{F_c[\eta_D(P_{in}/hf_m)\tau_{\text{int}}]^{1/2}}\right]\text{rad/s}\end{aligned} \tag{17}$$

where $\delta\Omega_{rms}$ is the rms, angular rotation rate, random walk error, η_D is the detector's quantum efficiency, h is Planck's constant, τ_{int} is the observation interval (i.e., detector integration time) and P_{in} is the total power launched bi-directionally into the ring, with half of the power propagating in each direction. Thus the accuracy of the passive resonant gyro can be improved by reducing the width of the resonance, $\delta\omega_{FWHM}$, or equivalently by increasing the finesse, F_c, of the ring resonator by reducing propagation losses in the ring. A resonant

#87963 - $15.00 USD Received 27 Sep 2007; revised 3 Dec 2007; accepted 5 Dec 2007; published 13 Dec 2007

optical gyroscope of ring perimeter L can, in theory, achieve the same shot noise-limited accuracy as a Sagnac-based interferometric fiber optic gyroscope of fiber length $LF_c/3$ [15]. This effective length enhancement by a factor of $F_c/3$ is the principal theoretical advantage of a resonant optical gyroscope as compared to a nonresonant, fiber-optic, interferometric gyroscope. The complexity of a resonant optical gyroscope, however, is considerably higher, and other parasitic effects, like Kerr nonlinearities, may make it difficult to achieve the fundamental performance limits given by Eq. (17).

The finesse of the resonator can be increased by including gain inside the ring to compensate for propagation loss. Fiber-based, active, ring resonators have been studied both theoretically and experimentally [20-22]. In the presence of gain, the ultimate accuracy of a resonant optical gyroscope will be limited by the spontaneous emission noise inside the ring rather than by shot noise at the detector. Using an analysis technique similar to that employed for ring laser gyroscopes [13], it will be shown below that, in the presence of gain, spontaneous emission noise limits the accuracy of a resonant optical gyroscope to a value given by

$$\delta\Omega_{rms} \approx \left(\frac{\lambda_m c}{4AN_{eff}}\right)\left[\frac{1}{\sqrt{F_c F_a}\,[(P_{in}/hf_m)\tau_{\text{int}}]^{1/2}}\right]\text{rad/s} \tag{18}$$

where F_c is the ("cold" cavity) finesse of the resonator in the absence of gain and F_a is the finesse when gain is present.

For simplicity, a number of assumptions will be made in our analysis. It will be assumed that the gain is produced by a transition between two levels of an atomic system, e.g., the $^4F_{3/2} \rightarrow {}^4I_{11/2}$ neodymium transition. The atomic population in the upper excited level ($^4F_{3/2}$) will be denoted by N_2, while the lower level ($^4I_{11/2}$) of the transition will be assumed to be unpopulated. The atomic transition will be assumed to be purely homogeneously broadened with a center transition frequency of f_a Hz (wavelength λ_a), a full-width-half-maximum linewidth of $\delta\omega_a$ rad/s, a stimulated emission cross-section of σ_e and a spontaneous emission lifetime of τ_{fl}. The losses in the resonator in the absence of gain will be assumed to be relatively low, and when gain is present, it will be assumed that the gain compensates nearly all of the propagation losses in the ring.

Let $< n >$ denote the average number of photons inside the ring cavity. Thus the strength of the electric field inside the cavity will be proportional to $\sqrt{< n >}$ and can be represented by vector as shown in Fig. 2 below. The angular position of the vector indicates the phase of the optical field.

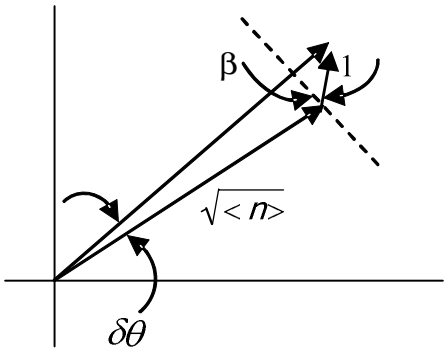

Fig. 2. Effect of spontaneous emission on frequency.

#87963 - $15.00 USD Received 27 Sep 2007; revised 3 Dec 2007; accepted 5 Dec 2007; published 13 Dec 2007

The short vector in Fig. 2 has a length of 1 and represents the spontaneous emission of a single photon from an excited atom of the gain medium into a single cavity mode. The angular orientation, β, of this vector relative to that the cavity mode signal vector is random and uniformly distributed over the interval [0, 2π). The addition of this spontaneously emitted photon changes the phase of the optical field in the cavity by δθ. Assuming that $< n > >> 1$, it may be concluded that

$$\delta\theta \approx \frac{1 \cdot \cos\beta}{\sqrt{< n >}} \tag{19}$$

and thus

$$< (\delta\theta)^2 > \approx \frac{1}{2 < n >} \tag{20}$$

Therefore the total change, $\delta\phi$, in phase of the optical signal field after M photons have been produced by M independent spontaneous emission events that occur in a time interval of duration τ_{int} will be given by

$$< [\delta\phi(\tau_{\text{int}})]^2 > \approx \frac{M(\tau_{\text{int}})}{2 < n >} \tag{21}$$

In a time interval of τ_{int} seconds the number of photons, $M(\tau_{\text{int}})$, that are spontaneously emitted into a single cavity mode is given by

$$M(\tau_{\text{int}}) = \frac{\tau_{\text{int}}}{\tau_{fl}} \frac{N_2}{s} \tag{22}$$

where s is the number of cavity modes in the ring resonator. Using the fact that the number of modes per unit volume per unit Hertz is given by [23]

$$\rho_b(f) = \frac{8\pi}{\lambda_a^2} \frac{n_r^3}{c} \tag{23}$$

where n_r is the refractive index of the ring. A homogeneous transition has the following Lorentzian spectral lineshape

$$S(f) = \frac{1}{1 + \left[\frac{2(f - f_a)}{\delta f_a}\right]^2} \tag{24}$$

and the area under this lineshape curve is equal to $\pi\delta f_a / 2$. It follows that

$$s = \frac{8\pi}{\lambda_a^2} \frac{n_r^3}{c} V \frac{\delta\omega_a}{4} = \frac{2\pi}{\lambda_a^2} \frac{n_r^3 V}{c} \Delta\omega_a \tag{25}$$

where V is the volume occupied by the ring resonator cavity and λ_a is the wavelength at the center of the atomic transition. The cold cavity photon lifetime, τ_p, is given by

$$\tau_p = \frac{n_r L / c}{1 - y^2 x^2} \tag{26}$$

#87963 - $15.00 USD Received 27 Sep 2007; revised 3 Dec 2007; accepted 5 Dec 2007; published 13 Dec 2007

and the reciprocal of the cold cavity photon lifetime is approximately equal to the full-width-half-maximum of the cold cavity resonance provided the resonator loss is small, i.e.,

$$\frac{1}{\tau_p} \approx \delta\omega_{FWHM} = \frac{2\pi c}{n_r L F_c} \tag{27}$$

where the second equality in Eq. (27) follows from Eq. (11). The round trip gain, G, in the ring is given by

$$G = e^{\sigma_e N_2 L/V} \approx 1 + \sigma_e N_2 L/V \tag{28}$$

It is assumed that the gain nearly compensates the resonator loss, and therefore the following condition is met

$$y^2 x^2 G \approx 1 \tag{29}$$

Combining Eqs. (26), (28)-(29) yields

$$N_2 \approx \frac{V}{\sigma_e L}(1 - x^2 y^2) = \frac{n_r V}{\sigma_e c}\frac{1}{\tau_p} \tag{30}$$

From the Einstein A and B relationship, it follows that [24]

$$\sigma_e = \frac{1}{2\pi}\frac{1}{\tau_{fl}}\frac{\lambda_a^2}{n_r^2 \Delta\omega_a} \tag{31}$$

The total optical power, P_c, in the resonator can be related to the average number of photons, $< n >$, in the resonator propagating in each direction by

$$< n > = \frac{n_r P_c L}{2 h f_a c} \tag{32}$$

Combining Eqs. (21)-(22), (25), (27) and (30)-(32) yields

$$< [\delta\phi(\tau_{\text{int}})]^2 > = \frac{2\pi\tau_{\text{int}} h f_a c^2}{F_c P_c n_r^2 L^2} \tag{33}$$

Now according to Eq. (14)

$$P_c \approx \frac{1}{\pi} F_a P_{in} \tag{34}$$

Also note that

$$\begin{aligned} &< [\delta f_{cw}]^2 > = < [\delta f_{ccw}]^2 > \\ &= < [\delta\phi(\tau_{\text{int}})]^2 > /(2\pi\tau_{\text{int}})^2 \end{aligned} \tag{35}$$

Combining Eqs. (33)-(35) yields the following expression for the frequency resolution of an active ring resonator in the quantum limit.

$$(\delta f_{cw})_{rms} = (\delta f_{ccw})_{rms} \approx \frac{c}{\sqrt{2} n_r L}\left[\frac{1}{\sqrt{F_a F_c}[(P_{in}/h f_a)\tau_{\text{int}}]^{1/2}}\right] \tag{36}$$

It follows from Eqs. (16) and (35) that

#87963 - $15.00 USD Received 27 Sep 2007; revised 3 Dec 2007; accepted 5 Dec 2007; published 13 Dec 2007

$$\delta\Omega_{rms} = <[\delta\Omega]^2>^{1/2} = \frac{\lambda_a L}{4\sqrt{2}\pi A\tau_{\text{int}}} <[\delta\phi(\tau_{\text{int}})]^2>^{1/2} \tag{37}$$

Combining Eqs. (33), (34) and (37) yields the final result for the gyro sensitivity in the quantum limit.

$$\begin{aligned}\delta\Omega_{rms} &\approx \left(\frac{\lambda_a c}{4An_r}\right)\left[\frac{1}{\sqrt{F_a F_c}[(P_{in}/hf_a)\tau_{\text{int}}]^{1/2}}\right] \\ &\approx \left(\frac{\lambda_a c}{4An_r}\right)\left[\frac{1}{F_c\sqrt{F_a/F_c}[(P_{in}/hf_a)\tau_{\text{int}}]^{1/2}}\right] \quad \text{rad/s}\end{aligned} \tag{38}$$

A comparison of Eqs. (17) and (38) indicates that in the quantum limit, the reduction in the rms, angular rotation rate, random walk measurement error is proportional to $1/\sqrt{F_a/F_c}$ rather than to $1/(F_a/F_c)$ when gain is included in the resonator ring. Thus doubling the finesse by using gain only reduces the quantum-limited measurement error by a factor of $\sqrt{2}$ rather than by a factor of 2.

Consider now the operation of the resonant optical gyroscope shown in Fig. 1 operating under the following conditions: (1) $K_{cw} = K_{ccw} \approx 0$, (2) the gain exactly cancels the propagation loss along the ring, i.e., $\rho_a = 0$, and (3) $\rho_c \approx 0$, where ρ_c and ρ_a denote the propagation loss coefficient, ρ, in the ring when gain is absent and present, respectively. It follows from Eq. (12) that

$$F_c \approx \frac{\pi}{1-(1-K_{cw})e^{-\rho_c L/2}} \approx \frac{2\pi}{\rho_c L} \tag{39}$$

and

$$F_a \approx \frac{\pi}{K_{cw}} \tag{40}$$

Therefore the inclusion of gain will reduce the rms angular rotation measurement error by a multiplicative factor equal to

$$\text{reduction factor} = \sqrt{\frac{F_a}{F_c}} \approx \sqrt{\frac{\rho_c L}{2K_{cw}}} \tag{41}$$

As a numerical example suppose the propagation loss in the ring, without gain, is 0.05 dB/cm, the ring diameter is 2 cm and the coupling coefficient is 0.1%, then $F_c \approx 86$, $F_a \approx 3140$ and the measurement error reduction factor due to the inclusion of gain is approximately 6. According to Eq. (41) an arbitrarily large improvement in performance should be attainable, in theory, by reducing the coupling coefficient, K_{cw}. According to Eqs. (34) and (40), however, the power, P_c, circulating in the ring at resonance is inversely proportional to K_{cw}. i.e.,

$$P_c = P_{in}/K_{cw} \tag{42}$$

where P_{in} is the power launched into the straight waveguides. Thus as K_{cw} is reduced, the power in the ring increases, and this in turn increases the gain saturation. Furthermore as the gain saturation increases additional pump power is required to maintain the required level of

#87963 - $15.00 USD Received 27 Sep 2007; revised 3 Dec 2007; accepted 5 Dec 2007; published 13 Dec 2007

loss compensation, i.e., $\rho_a = 0$. An expression for the required absorbed pump power is derived below

$$\sigma_e N_2^{(sat)} \approx \rho_c \tag{43}$$

$$N_2^{(sat)} \approx \frac{N_2^{(unsat)}}{1 + 2P_c / P_{sat}} \tag{44}$$

$$P_{sat} \approx \frac{hf_a}{\sigma_e \tau_{fl}} A_{wg} \tag{45}$$

where A_{wg} is the cross-sectional area of the ring waveguide. Eq. (43) expresses the condition that the gain compensates the losses in the ring, i.e., $\rho_a = 0$, Eq. (44) is the relationship between the saturated and unsaturated (i.e., when $P_{in} = 0$) population in the upper level, and P_{sat} is the saturation power of the gain transition. The absorbed pump power, Pp, at wavelength λ_p required to maintain an unsaturated upper level population, $N_2^{(usat)}$, is given by

$$P_p = \frac{hc / \lambda_p}{\tau_{fl}} N_2^{(usat)} A_{wg} L \tag{46}$$

Combining Eqs. (41)-(46) and invoking the fact that $P_c >> P_{sat}$ when the gain is highly saturated yields the following final result for the required absorbed pump power.

$$P_p \approx 4 \frac{\lambda_a}{\lambda_p} \frac{F_a}{F_c} P_{in} \tag{47}$$

4. Fabrication and experimental results

A prototype active ring resonator was designed and fabricated in an ion-exchangeable silicate glass doped with 2 weight percent Nd_2O_3. The ring resonator consists of a pair of straight waveguide arms, a pair of directional couplers and a racetrack ring as shown in Fig. 3.

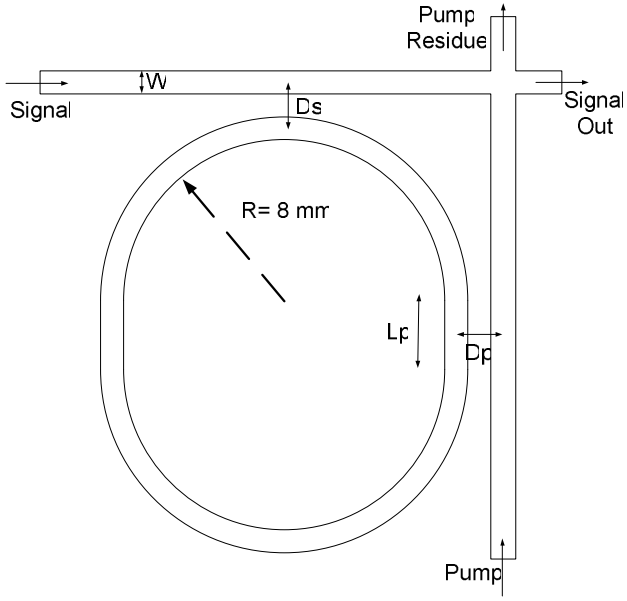

Fig. 3. Mask layout for single-arm racetrack active ring resonator with pump coupler.
W = 1.3 μm, D_s= 8.4 μm, L_p = 2.915 mm, D_p = 7.55 μm

#87963 - $15.00 USD Received 27 Sep 2007; revised 3 Dec 2007; accepted 5 Dec 2007; published 13 Dec 2007

The racetrack consists of two half circles of radii 8 mm joined together by two 2.915 mm long straight sections. For the directional couplers, the fraction of power coupled from the signal arm into the ring at the signal and pump wavelengths is given by $K_s(\lambda_s)$ and $K_s(\lambda_p)$, respectively, while $K_p(\lambda_s)$ and $K_p(\lambda_p)$ denotes the corresponding coupling coefficients for the pump arm. In order to achieve a high finesse at moderate launched pump powers, the couplers should have small values for $K_s(\lambda_s)$, $K_p(\lambda_s)$ and $K_s(\lambda_p)$, while $K_p(\lambda_p)$ should be kept as close to one as possible. Given that the gain medium was chosen to be neodymium-doped glass, $\lambda_s \approx 1060$ nm and pumping can be accomplished using a laser diode operating at a wavelength of $\lambda_p \approx 830$ nm.

E-beam evaporation was used to deposit a 150 nm thick layer of titanium onto the glass substrate, and then a conventional photolithographic process was utilized to pattern the titanium layer according to the layout shown in Fig. 3. During silver ion exchange, metallic silver clustering can occur at the edges of the titanium mask openings resulting in large propagation losses. In order to mitigate this effect, the titanium mask was oxidized by placing the wafer in a pure $NaNO_3$ melt at 330°C for one hour. After this step, the ion exchange was performed in a mixed melt of silver nitrate and sodium nitrate (0.35 mol%:99.65 mol%) at 320° C for 15 minutes. Following the exchange, the titanium mask was removed, the waveguide edges were polished and the sample was cleaned. The device was subjected to four cycles of thermal annealing, each of 5 minute duration at a temperature of 320°C. The un-pumped spectral response of the device was measured after each annealing step using a tunable, external cavity, diode laser manufactured by New Focus operating with a linewidth below 300 KHz. From these measurements, finesse and dip values were found. The pump coupler efficiencies, $K_p(\lambda_p)$ and $K_p(\lambda_s)$, were also measured using separate sets of test couplers that were fabricated together with the resonator on the same chip. The finesse and dip values, along with knowledge of $K_p(\lambda_s)$, allowed us to compute the values of ρ and $K_s(\lambda_s)$. During the thermal annealing steps, diffusion causes the previously indiffused Ag^+ ion concentration profile to increases in width and depth, decrease in peak magnitude and assume a smoother shape. These changes reduce the propagation losses due to scattering, but increase the bending loss due to a reduction in Δn. The overall propagation loss is minimized for some optimal amount of thermal annealing [9]. The coupling efficiencies of the directional coupler will also change as the device is annealed, and these efficiencies are very sensitive to changes in the refractive index profile, thus making accurate design work difficult. Based on our previous experience fabricating passive ring resonators in un-doped version of a similar glass and the corresponding measured refractive index profiles of these devices, the mask parameters specified in Fig. 3 were chosen [9]. Coupled mode calculations indicated that these parameters should yield small values for $K_s(\lambda_s)$, $K_p(\lambda_s)$ and $K_s(\lambda_p)$ and a relatively large value for $K_p(\lambda_p)$. Several devices with different pump coupler interaction lengths, L_p, were fabricated, thus allowing us to select the device that achieved the most favorable values for $K_p(\lambda_p)$ and $K_p(\lambda_s)$, while simultaneously obtaining low values for $K_s(\lambda_s)$ and $K_s(\lambda_p)$. In the absence of pumping, the measured finesse and dip of the final device were found to be 10.8 and 6.2%, respectively. From these measured values, the propagation loss, ρ, and the coupling efficiency, $K_s(\lambda_s)$, for the signal were deduced to be 0.45 dB/cm and 0.94%, respectively. $K_p(\lambda_p)$ and $K_p(\lambda_s)$ were measured to be 52.3% and 3.5%, respectively, using separate sets of test couplers as described above. The high propagation loss for the device reported here is likely due to the small volume of the glass melt used to produce the Nd-doped substrates. Smaller volume melts often result in glasses of lower optical quality. Using similar ion exchange processing, propagation losses on the order of 0.1 dB/cm have been obtained in the un-doped, commercially available version of a similar glass [9]. Losses on the order of 0.01 dB/cm have been achieved for slightly larger sized rings using CVD-deposited silica on silicon films and patterning using RIE [10]. The use of RIE patterning together with such a

#87963 - $15.00 USD Received 27 Sep 2007; revised 3 Dec 2007; accepted 5 Dec 2007; published 13 Dec 2007

material system would also simplify the coupler design process and enhance the ability to repeatedly fabricate nearly identical devices.

The output of a 150 mW, single spatial mode, TE-polarized, laser diode operating in the vicinity of 830 nm was coupled into the pump arm of the device described above as shown in Fig. 3. The spectral response of the resonator was measured using the New Focus tunable source, and the results are shown in Fig. 4. A long-pass filter, having a cut-off near 900 nm, and a narrow bandpass filter centered at the signal wavelength were placed between the output of the signal arm and the detector in order to remove the residual pump signal and spontaneous emission noise, respectively. The measured, off-resonance, signal power level at the detector during this measurement was 1.7 μW. The spectral response shown in Fig. 4 corresponds to a free-spectral range (FSR) of 3.8 GHz, a full-width-half-maximum resonance bandwidth of 15 MHz, a finesse of 250 and a dip of 89%. Using these finesse and dip values, $K_s(\lambda_s)$ and the effective propagation loss inside the ring (including signal loss at the pump coupler) was computed to be 0.84% and 0.013 dB/cm, respectively.

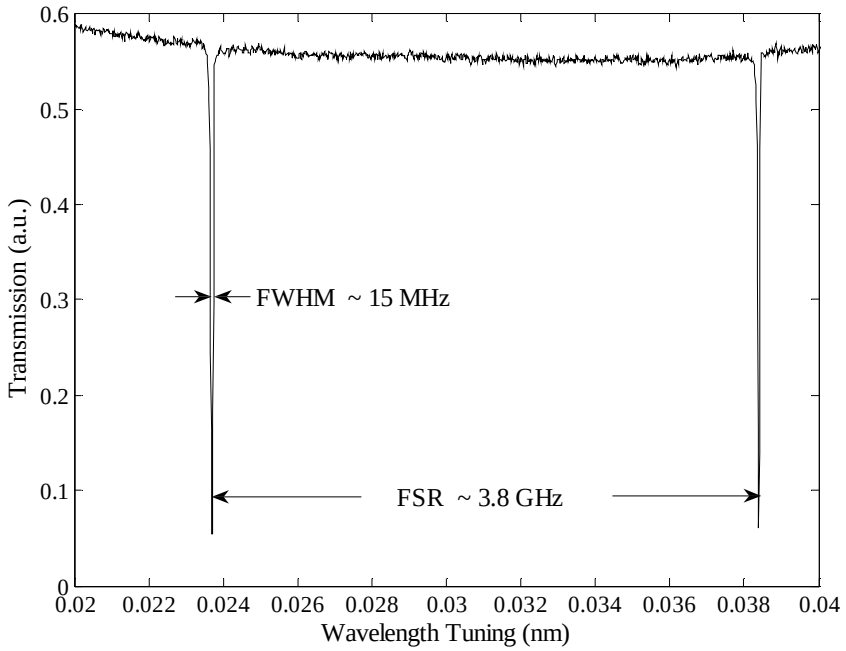

Fig. 4. Spectral response of active ring resonator.

Spectral measurements were repeated at a variety of laser diode pump powers and the results are shown in Fig. 5. As expected, the effective loss decreases and the finesse increases as the pump power is increased.

#87963 - $15.00 USD Received 27 Sep 2007; revised 3 Dec 2007; accepted 5 Dec 2007; published 13 Dec 2007

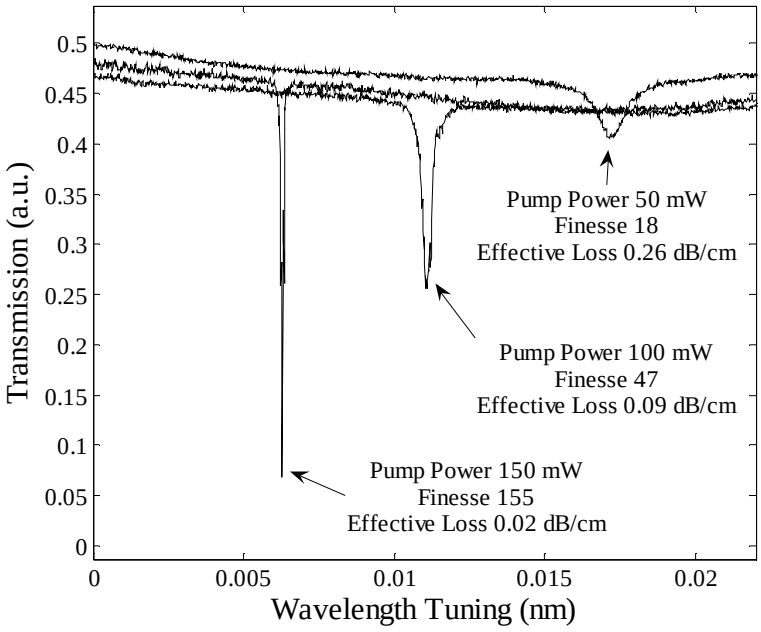

Fig. 5. Spectral response of active ring resonator as a function of pump power at fixed signal power.

At a fixed pump power, a decrease in finesse due to gain saturation was also observed as more signal power was coupled into the ring. These gain saturation results are shown in Fig. 6 as a function of the output signal power measured off-resonance at the detector.

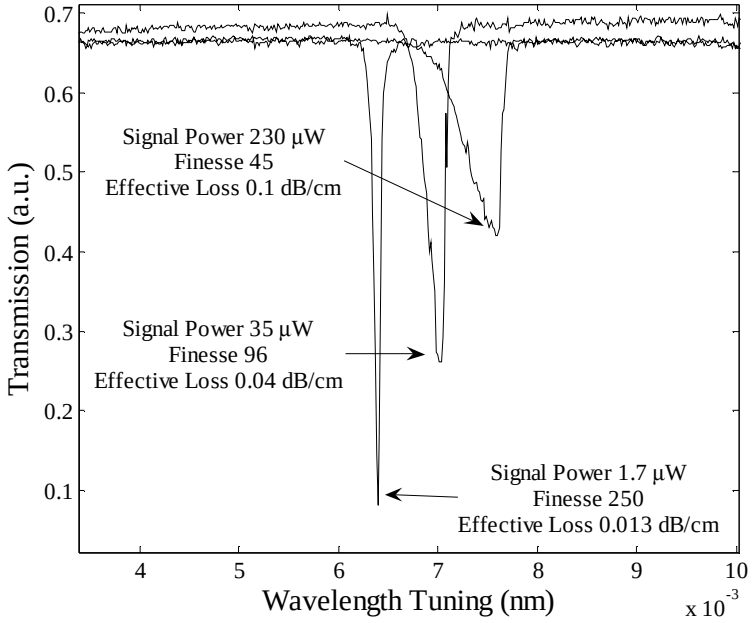

Fig. 6. Spectral response of active ring resonator as a function of signal power at fixed pump power.

#87963 - $15.00 USD Received 27 Sep 2007; revised 3 Dec 2007; accepted 5 Dec 2007; published 13 Dec 2007

Without any launched input signal, the pump power at the device input was increased. A plot of the output signal power, measured at the pump output port, versus input pump power is shown in Fig. 7. The output signal power vs input pump power curve shows an abrupt slope change at 110 mW indicating the onset of lasing.

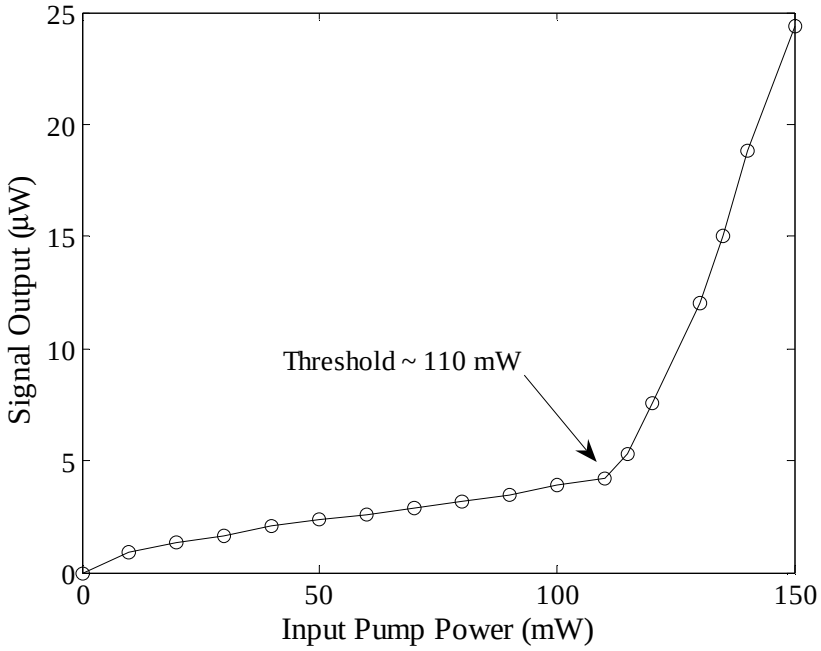

Fig. 7. Lasing characteristic.

The high pump power required to achieve lasing can be attributed to high losses in the passive ring resonator together with poor coupling from the diode pump laser into the straight-arm of the pump waveguide. Thus it was difficult to achieve lasing with our pump diodes and unwanted laser action was not observed. In general, however, the launched pump and/or signal powers may need to be carefully controlled in order to inhibit lasing. The spectral analysis performed in section 3 assumed a purely homogeneously-broadened transition and thus a population inversion that saturates uniformly across the gain transition. If the transition is inhomogenously-broadened, then to first order only the spontaneous emission originating from the homogeneously-broadened spectral packet lying closest to the launched signal's frequency will limit the frequency resolution. Consequently, the basic results Eqs. (36) and (38) will remain unchanged. When operated as a resonant optical gyro, lasing must be prevented. Because of spectral hole burning, however, the signal inside the resonator may only inhibit lasing at the cavity modes in the vicinity of the signal frequency. In order to inhibit the more distant spectral modes from lasing, it may be necessary to incorporate a course spectral filter into the cavity.

5. Conclusions

In summary, the ultimate spectral resolution obtainable using an active ring resonator is limited by spontaneous emission noise in the gain medium. An expression is derived for this quantum-limited resolution, and the result is applied to determine the fundamental performance limit of a resonant optical gyroscope implemented using a active ring resonator. With the addition of gain, the rms, angular rotation rate, random walk error is shown to decrease by a multiplicative factor equal to the square-root of the ratio of the resonator finesse

#87963 - $15.00 USD Received 27 Sep 2007; revised 3 Dec 2007; accepted 5 Dec 2007; published 13 Dec 2007

measured with gain and without gain present. An active, integrated optic, ring resonator is fabricated in a Nd-doped glass by ion exchange. When the gain medium is pumped, the finesse of the 1.6 cm diameter ring resonator is observed to increase from approximately 11 to 250.

Acknowledgements

This work was partially supported by the Office of Naval Research award no. N00014-05-1-0125. Special thanks are due to Dr. Joe Hayden of Schott Glass and Dr. Shibin Jiang of NP Photonics who provided ion exchangeable, rare-earth doped, glass substrates for this work.

#87963 - $15.00 USD Received 27 Sep 2007; revised 3 Dec 2007; accepted 5 Dec 2007; published 13 Dec 2007